

Title page:

## Mechanical wave velocities in left ventricular walls – in healthy subjects and patients with aortic stenosis

Word count (text (introduction – conclusions), references and figure legends): 4981/5000. (Perspectives 153)

### Authors:

Torvald Espeland, MD<sup>a,c</sup> – [torvald.espeland@ntnu.no](mailto:torvald.espeland@ntnu.no)

Morten S. Wiggen, PhD<sup>b</sup> - [morten.s.wiggen@ntnu.no](mailto:morten.s.wiggen@ntnu.no)

Havard Dalen, MD<sup>a,c,d</sup> – [havard.dalen@ntnu.no](mailto:havard.dalen@ntnu.no)

Erik A. R. Berg, MD<sup>b,c</sup> - [erik.a.berg@ntnu.no](mailto:erik.a.berg@ntnu.no)

Tommy A. Hammer, MD<sup>a,e</sup> - [tommy.arild.hammer@stolav.no](mailto:tommy.arild.hammer@stolav.no)

Sebastien Salles, PhD<sup>b</sup> - [sebastien.salles@ntnu.no](mailto:sebastien.salles@ntnu.no)

Lasse Lovstakken, PhD<sup>b</sup> - [lasse.lovstakken@ntnu.no](mailto:lasse.lovstakken@ntnu.no)

Brage H. Amundsen, MD, PhD<sup>a,c</sup> - [brage.hoyem.amundsen@stolav.no](mailto:brage.hoyem.amundsen@stolav.no)

Svend Aakhus, MD, PhD<sup>a,c</sup> - [svend.aakhus@ntnu.no](mailto:svend.aakhus@ntnu.no)

- a) Department of Circulation and Medical Imaging, Faculty of Medicine and Health Sciences,  
Norwegian University of Science and Technology (NTNU), Trondheim, Norway

- b) Centre for Innovative Ultrasound Solutions, Department of Circulation and Medical Imaging,  
Faculty of Medicine and Health Sciences, NTNU, Trondheim, Norway
- c) Clinic of Cardiology, St. Olavs hospital, Trondheim University Hospital, Trondheim, Norway
- d) Department of Internal Medicine, Levanger Hospital, Nord-Trøndelag Hospital Trust, Levanger,  
Norway
- e) Department of Radiology, Clinic of Radiology and Nuclear Medicine, St. Olavs hospital,  
Trondheim University Hospital, Trondheim, Norway

Conflict of interest / financial disclosures: GE Vingmed Ultrasound provided a Vivid E95 ultrasound scanner for research purposes for this project without any restrictions on design of the study or its publication. As a group we do not have any other conflict of interest or financial disclosures to declare in relation to this manuscript.

Address for correspondence:

Torvald Espeland

phone: +47 997 03 156, e-mail: [torvald.espeland@ntnu.no](mailto:torvald.espeland@ntnu.no), no twitter account

NTNU, Faculty of Medicine and Health Sciences, Department of Circulation and Medical Imaging,  
Postbox 8905, 7491 Trondheim, Norway

Running title: Mechanical wave velocities in LV-walls

## Acknowledgements

We appreciate the contributions from clinical research nurses Eli Granviken (Master in Clinical Nursing, Operating room nursing) and Marit Inderhaug Husby (Master in Clinical Nursing, Critical care nursing) in data collection.

## Short tweet:

Evaluation of myocardial structure using high frame rate echocardiography is feasible and can discriminate patients with aortic stenosis from healthy subjects

#cvImaging #cvEcho #Highframerate #aorticstenosis

## Structured abstract

Word count: 247/250

### Background:

Mechanical wave velocity (MWV) measurement is a promising method for evaluating myocardial stiffness, as these velocities are higher in patients with myocardial disease.

### Objectives:

Using high frame rate (HFR) echocardiography and a novel method for detection of myocardial mechanical waves, this study aimed to estimate the MWVs for different left ventricular walls and events in healthy subjects and patients with aortic stenosis (AS). Feasibility and reproducibility were evaluated.

### Methods:

We included 63 healthy subjects and 13 patients with severe AS. All participants underwent echocardiographic examination including 2D HFR recordings using a clinical scanner. Cardiac MRI was performed in 42 subjects. We estimated the MWVs at atrial kick (AK) and aortic valve closure (AVC) in different LV walls using the *clutter filter wave imaging* method.

### Results:

Mechanical wave imaging in healthy subjects demonstrated the highest feasibility for the AK-wave reaching >93 % for all four examined LV walls. The MWVs were higher for the infero- and anterolateral walls (2.2 and 2.6 m/s), compared with infero- and anteroseptal walls (1.3 and 1.6 m/s) ( $p < 0.05$ ) among healthy subjects. The septal MWVs at AVC were significantly higher for patients with severe AS than for healthy subjects.

Conclusions:

MWV estimation during AK is feasible and demonstrates higher velocities in the lateral walls, compared with septal walls. We propose indicators for quality assessment of the mechanical wave slope, as an aid for achieving consistent measurements. The discrimination between healthy subjects and patients with AS was best for the AVC mechanical waves.

Keywords:

Left ventricle, natural mechanical waves, myocardial stiffness, myocardial fibrosis, high frame rate imaging, echocardiography

## Condensed abstract

Word count: 89/100

We examined 63 healthy subjects and 13 patients with severe aortic stenosis (AS) with echocardiography including high frame rate imaging and cardiac MRI. In healthy subjects, mechanical wave velocity (MWV) estimation was feasible, but demonstrated varying velocities depending on left ventricular (LV) wall and cardiac cycle event. We propose quality indicators for systematic evaluation of the mechanical wave slope. Recordings of the atrial kick wave in different LV walls demonstrated excellent feasibility and high reproducibility. In AS patients, MWVs at aortic valve closure were higher than among healthy subjects.

## Abbreviations list

<b>Abbreviation</b>	<b>Meaning</b>
A4C	Apical 4-Chamber
AK	Atrial kick / contraction
AS	Aortic stenosis
AVC	Aortic valve closure
CMR	Cardiac magnetic resonance imaging
HFR	High frame rate
LV	Left ventricle / ventricular
MVC	Mitral valve closure
MWV/MWVs	Mechanical wave velocity/-ies
PLAX	Parasternal long axis

## Text

### Introduction

Various cardiac diseases cause fibrotic replacement of muscular tissue, potentially leading to heart failure, ischemia, or arrhythmia. Both subtype and amount of fibrosis influence outcome (1,2). Histopathology is the gold standard for evaluation of myocardial fibrosis (2). Cardiac Magnetic Resonance imaging (CMR) is considered the non-invasive reference for such evaluation and facilitates tissue characterization through detection of late gadolinium enhancement, native T1-mapping, and estimation of extracellular volume (1,2). However, the physiological implications of myocardial fibrosis are not easily evaluated by CMR.

By application of multiline reception and broad transmit beams, echocardiography can achieve very high temporal resolution (>500-1000 frames/s) for broad sectors, enabling imaging of short-lived cardiac events (3). Myocardial mechanical waves can be induced by an external force or by intrinsic cardiac events during the cardiac cycle, such as atrial contraction/kick (AK) or mitral and aortic valve closure (MVC and AVC). The valve closure waves occur during isovolumic phases, with limited left ventricular (LV) deformation, but rapidly changing myocardial tension. These two waves are presumably shear (transverse) waves, propagating orthogonally to the local particle displacements, at velocities up to 10 m/s in healthy individuals (3-6). Recent insight suggests that the AK-wave is a pressure wave (7).

Previous studies analyzing shear waves have indicated a time dependency of myocardial stiffness, reaching its maximum in systole. Changes in geometry and load explain physiological variation during the cardiac cycle (5,6,8-11). Shear wave velocities have previously been related to ageing, cardiac morphology, contractility, and diastolic myocardial stiffness (3,8-10,12-16).



The method appears clinically relevant, since numerous trials have demonstrated higher mechanical wave velocities (MWVs) in various cardiac disorders, such as post cardiac transplantation, hypertensive and hypertrophic cardiomyopathy, cardiac amyloidosis, valvular heart disease, and ischemic heart disease (5-7,9-15,17,18).

We have developed a new ultrasound method, to detect myocardial mechanical waves, termed *clutter filter wave imaging*, which detects mechanical wave propagation without prior motion estimation (19). An appropriate wall filter highlights the motion induced by the mechanical event, displaying the wave propagating as either red or blue regions across the B-mode and the corresponding anatomic M-mode images. The method has been implemented on a high-end clinical ultrasound scanner. Compared with tissue Doppler, the method appears more consistent and sensitive to subtle tissue displacements, and improves AK-wave visualization in both lateral and septal walls (19).

By applying mechanical wave imaging in healthy individuals and patients with severe aortic stenosis (AS) we aimed to 1) evaluate the feasibility for detecting naturally occurring mechanical waves, 2) measure the corresponding MWVs in different LV walls, and 3) evaluate the reproducibility of these measurements in healthy subjects.

## Methods

### Study population

We recruited 31 healthy volunteers and 13 patients with severe AS from the clinical trial *Ultrasonic Markers for Myocardial Fibrosis and Prognosis in Aortic Stenosis* (ClinicalTrials.gov ID: NCT03422770) (Population-StOlav). The study was approved by the Regional Committee for Medical and Health Research Ethics. All subjects provided informed written consent. Exclusion criteria were estimated glomerular filtration rate  $<30$  ml/min/1.73m<sup>2</sup>, previous myocardial infarction and conditions (except aortic stenosis) known to cause significant myocardial fibrosis, such as deposition disorders, cardiomyopathies, poorly treated hypertension or diabetes, and former thoracic radiation. Patients with CMR contraindications, chronic atrial fibrillation, significant frailty, or short life expectancy were not included. In addition, we included 34 subjects defined as healthy with available HFR-recordings from the fourth wave of the Trøndelag Health (HUNT4) study (Population-HUNT) (Table 1). These subjects had no known hypertension, diabetes, cancer, or cardiac or pulmonary disease (20).

### Echocardiography

An experienced echocardiographer (TE) acquired 2D and 3D images using a Vivid E95 clinical scanner (GE Vingmed Ultrasound, Horten, Norway) and the M5Sc, 4V and 4Vc probe in Population-StOlav. De-identified data were analyzed offline using Echopac 204.41.1 (GE Vingmed Ultrasound) according to current recommendations (21,22). Using the same scanner, 2D-HFR images were acquired from the parasternal long axis (PLAX) and apical four chamber (A4C) view using the 1.5D M5Sc-D cardiac probe with a 3.5 MHz central frequency. HFR was achieved by transmitting 6 non-overlapping diverging waves with receive beamforming of a sector of 10° per transmit, resulting in a fixed image sector of 60° and 12 cm depth. We acquired

2-4 complete cardiac cycles per view. The echocardiographic studies in Population-HUNT were performed by two experienced sonographers. Here, A4C 2D HFR data were acquired from 1–2 cardiac cycles with a similar set-up, but with an adjustable sector size aimed to include the complete LV with the highest possible frame rate (Table 1).

#### HFR-analysis

The mechanical wave propagation was detected using *clutter filter wave imaging*, which employs a specific clutter filter to attenuate background myocardial velocities and thus enhance the motion induced by moving mechanical waves. The cut-off frequency was set to 91 Hz to attenuate tissue velocities  $<2.0$  cm/s (17,19). The waves were further enhanced by calculating the temporal derivative which produces an acceleration map. This map was smoothed spatially (10 x 10 spatial samples) and temporally (35 ms). The mechanical wave propagation was analyzed offline using an in-house-developed dedicated software (PyMWI). Pulsed wave Doppler at the base of the respective wall was used for timing purposes. The M-mode line was placed in the mid-myocardium at the designated cardiac event, excluding the membranous septum. On the created M-mode map, the slope of the mechanical wave was manually drawn in the middle of the wave (Central Illustration). Waves originating in the basal LV at the following time points were isolated:

1. The AVC-wave originating during early isovolumetric relaxation
2. The AK-wave arising in the early phase of atrial contraction

Initial evaluation of AK-, MVC- and AVC-waves indicated that MVC-waves and lateral AVC-waves were more difficult to distinguish from noise with our setup. We therefore studied the infero- and anteroseptal AVC-waves and the AK-waves in all four walls covered by the A4C and PLAX view. Wave quality was evaluated, and at each event, the MWV was measured

manually, as given by the slope of the propagation along the M-mode line (Central Illustration). To evaluate reproducibility, the analyses were repeated in 20 randomly selected healthy subjects 3 months later by the same observer (intraobserver), and by a second observer (interobserver).

#### Cardiac MR Imaging

CMR was performed on a Siemens 3T Prisma (Siemens, Erlangen, Germany). A short-axis stack of balanced steady-state free precession images was acquired for analysis of LV mass and volumes. A gadolinium-based contrast agent (Gadobutrol 0.15 mmol/kg) was administered to evaluate late gadolinium enhancement and extracellular volume. T1-mapping pre- and 10 minutes post-contrast was achieved using the MODified Look-Locker Inversion (MOLLI) recovery sequence. Three short-axis slices were acquired at the basal to midventricular level (spatial resolution 1.4 x 1.4 mm, slice thickness 8 mm and gap 1.6 mm). LV mass, volumes, late-enhancement, and T1-mapping including extracellular volume were determined according to current recommendations (23,24). Specifically, 2 – 3 regions of interest in the basal to midventricular septal region were selected for T1-mapping. Image analysis was performed by one observer (TE) blinded for clinical information using the Segment version 3.0 R7946 (Medviso, Lund, Sweden) (25).

#### Statistical analysis

Continuous variables are presented as mean  $\pm$  SD if normally distributed, otherwise as median and interquartile range. Categorical data are expressed as numbers and percentages. Normal distribution was evaluated by histograms, QQ-plots and the Shapiro-Wilk test. For comparisons of mean or median values, T-test or Mann Whitney U test was performed, respectively. A 2-sided p-value  $<0.05$  was considered statistically significant. The associations between variables

are expressed using the Pearson or Spearman correlation coefficients. Reproducibility was evaluated using intraclass correlation and Bland Altman statistics. Data were processed and analyzed in Microsoft Excel (Microsoft, Washington, USA) and SPSS 28.0 (IBM, New York, USA).

## Results

### Study population

Due to asymptomatic cardiac disease detected on CMR, 2 presumed healthy participants were excluded from Population-StOlav. Baseline characteristics, biochemical parameters and imaging findings are presented in Table 2 and 3. All were Caucasian and presented with sinus rhythm. Compared with the healthy subjects, patients had significantly higher NT-proBNP, thicker LV walls, increased LV-mass, reduced longitudinal shortening, more prevalent diastolic dysfunction and larger and less compliant left atria. Native T1 values and extracellular volume were within normal ranges for a 3T magnet in the healthy subjects, the former was increased in patients (Table 3). Late gadolinium enhancement was present in 4 patients (31%). The Population-HUNT were somewhat younger and healthier than Population-StOlav (20).

### Quality of mechanical wave detection and feasibility

Each wave was rated according to specified rules, forming 8 different rating categories (Table 4). Waves with rating  $\geq 4$  were included in the final analysis. In Population-StOlav, for each wall and event, 2-4 waves were visualized per subject, depending on heart rate and timing of acquisition. Among healthy subjects in Population-StOlav, 85% of the waves were accepted for further analyses (Table 4) and all walls demonstrated  $>93\%$  acceptance rate for the AK-wave (Table 5A). For patients, a lower acceptance rate was observed for the AK-wave in the anteroseptal and anterolateral walls. Additionally, compared with the PLAX view, the traced velocity slope was systematically longer in the apical view for both examined events (Table 5A).

## MWV across walls and events

The AK-MWVs were higher in the antero- and inferolateral LV walls compared with the antero- and inferoseptal walls (Figure 1 and Table 5B). For the inferoseptal wall, the MWVs were higher at AVC than at AK.

## Reproducibility

Reproducibility was examined in healthy subjects from Population-StOlav. Intra- and interobserver variation values were in general good to very good and similar for all walls and events (Figure 2 and Table 6). Despite a small sample size, it is worth noticing that intraclass correlation was lowest for inferoseptal AVC and anteroseptal AK MWVs both for intra- and interobserver analysis.

## MWV in AS

Patients with severe AS demonstrated 62 % higher AVC-MWVs in both examined septal walls (Table 5B and Figure 3). Furthermore, their AK-MWVs were higher in all LV walls, but not significant. The MWVs were most homogenous for the inferoseptal AK-wave.

## Comparisons to clinical and imaging parameters

In general, associations between the different MWVs and imaging parameters were weak. Peak jet velocity across the aortic valve demonstrated clear positive correlation to MWVs in both the antero- and inferoseptal wall ( $r=0.42, p=0.035$ ;  $r=0.47, p=0.013$ ). A weak positive association between MWV at AVC in the anteroseptal wall and CMR-measures was observed (Figure 4a and 4b). Furthermore, compared with healthy subjects (Population-StOlav), the patients demonstrated a larger delay from the start of the septal a'-wave to the initiation of the AK-wave propagation in the same region ( $38\pm6$  ms vs.  $32\pm7$  ms,  $p=0.022$ ).

MWV in the HUNT-study

Median frame rate was 1403 (1213–1619)/s, compared with  $858 \pm 0$ /s in Population-StOlav (Table 1). Population-HUNT demonstrated similar MWVs as the healthy subjects in Population-StOlav (Table 5b).



## Discussion

This study demonstrates that LV myocardial mechanical waves originating from AVC and AK can be recorded in healthy subjects and patients with AS using the *clutter filter wave imaging* approach and a commercially available echocardiographic scanner. Among healthy subjects, the feasibility for measuring the AK-MWV was excellent, and better than for AVC. Furthermore, higher MWVs were found in the two LV lateral walls. Interobserver reproducibility was good, and similar to intraobserver assessment. Patients with severe AS demonstrated higher MWVs at AVC compared with healthy subjects.

### Study population

The healthy subjects in the present study were older and had higher systolic blood pressure and body mass index than in similar previous studies, likely making them more comparable to cardiac patients (11,14,16,26). An ageing healthy population might have minor changes in myocardial properties, possibly affecting the propagation of mechanical waves. In Population-StOlav, we included healthy subjects with well-controlled hypertension and diabetes displaying important biochemical and imaging parameters within normal ranges (Table 2) (11,16,18). We believe this population may serve as a comparison to a population with cardiac disease.

### MWV by clutter filter wave imaging

This is the first clinical study presenting 2D MWVs in healthy subjects and patients with severe AS using the *clutter filter wave imaging* approach, which enhances the mechanical waves of interest. Furthermore, we systematically evaluated and provided MWV estimates for the natural waves originating from AVC (septum) and during AK both in the septal and lateral walls.

## Quality of mechanical wave detection and feasibility

Quality indicators for evaluating the mechanical waves have been proposed (27), but never systematic evaluated. We believe criteria as suggested in table 4 can be applied in formulating general recommendations for consistent and robust application of this technique. Table 7 provides an overview of MWVs in previous studies, depending on acquisition, view, and LV wall at different events during the cardiac cycle in healthy and disease (5-7,10,11,13-18,26-31).

We obtained a frame rate of 858/s in Population-StOlav, and 1406/s in Population-HUNT, the highest reported frame rate for similar applications on a clinical scanner (4,5,10) (Table 1 and 7). A frame rate of 858/s yields a temporal resolution of 1.16 ms. Thus, a MWV of 5.0 m/s would correspond to a propagation distance of 5.8 mm per frame. A slower propagating wave will demonstrate a smoother wave front, due to more frequent registrations. The M-mode line length is an important quality indicator, as a shorter line results in fewer observations (6). For proper evaluation of faster waves ( $>4$  m/s), like AVC waves in patients, higher frame rates should be targeted.

The AK-wave was better visualized than the AVC-waves in most subjects across the examined walls. The inferoseptal and inferolateral AK-wave had the highest proportion of accepted waves and the highest quality ratings. Our method was specifically optimized for detecting AK-waves, and technical optimization of the *clutter filter wave imaging* method may improve results for other events. The very high feasibility for the AK-wave is concordant with previous studies (7,10,11,17,19). The feasibility for detection of the AVC wave has previously been reported higher than the MVC wave (5,14,26).

In some individuals, we observed a local velocity change, notching, of the mechanical wave (Table 4 – rating 7). This could be caused by signal noise, focal myocardial stiffness variation (fibrosis or other causes of tissue anisotropy), changing geometry or load, or by the wave propagating out of the image plane or entering the plane from another direction, all affecting the estimated MWV (30). Three-dimensional imaging may clarify if notching is caused by altered cardiac structure or out of plane wave propagation. Rating 2 with the bidirectional waves might be explained by waves propagating in different parts of the LV with different velocities (higher in the lateral wall) and then interfering in the more apical regions of the septum. This is supported by observations from initial 3D-studies. M-line crossing of stitches in the 2D B-mode image explains explain the artifacts corresponding to rating 5. Furthermore, varying thickness of the lines and timing issues may create challenges in the automatization of the analysis process, especially in recordings with poor PW Doppler spectrum quality.

#### MWV across walls and events

In Population-StOlav healthy subjects we report average AK-wave velocities ranging from 1.3–2.5 m/s, comparable to previous reports of 1.1–2.4 m/s for similar LV walls (Tables 5b and 7) (6,10,11,16,17,31). A research group has previously presented an average AK-MWV recorded from the three apical views (11,16,18). For healthy subjects, the reported MWV after AVC of 1.9–2.4 m/s in the two examined walls was lower than previously reported, mainly 3.0–4.0 m/s (5,14,26). Prior studies have mainly used the PLAX view and Tissue Doppler Imaging for evaluating the mechanical waves (Table 7) (6).

In the PLAX and A4C-views, recordings covered both septal and lateral walls, hereby omitting variation caused by differences in cardiac cycle duration and beat-to-beat variation in load. For

healthy subjects, the AK-MWVs were significantly higher in the lateral walls, compared with septum. This might be explained by different boundary conditions from the right ventricle compared with the pericardium, with wall thickness and radius of the myocardial wall curvature potentially modulating this effect (13).

As atrial contraction occurs during low intraventricular pressure and wall stress, the AK-wave may provide important information about myocardial properties and stiffness (10,11,32). AK-MWVs are associated with increased major adverse cardiac events, including death (11,16,18). The AK-wave is absent in atrial fibrillation and may be affected by other arrhythmias, increased LV filling pressure and atrial dysfunction.

Conversely, the MVC- and AVC-waves might be affected by valvular heart disease. At AVC, in contrast to AK, higher MWVs are explained by a contracted myocardium and an increased load (5,6,14). We found low correlation between MWVs from different LV walls and events.

Specifically, in healthy subjects, the AVC MWV was higher in the inferoseptal wall, and the correlation between the inferoseptal (A4C) and anteroseptal wall (PLAX) was not significant (Figure 1). This lack of correlation supports a previous study indicating that a combination of imaging views may provide supplementary information about myocardial properties, and that different MWVs in septal regions from A4C and PLAX may be explained by the AVC force consisting of both transversal and longitudinal components (29). Summarized, the population characteristics, sample size and the method for mechanical wave imaging and analysis should all be considered when comparing trials.

#### Reproducibility

Reproducibility for all LV walls was comparable to other studies (11,14,26,27). For the inferoseptal wall, AK-MWVs demonstrated excellent intra- and interobserver variation (Figure 2

and Table 6). Interestingly, lower reproducibility was detected in the two walls, inferoseptal (A4c) and anteroseptal (PLAX), where the initial wave propagation is incompletely covered. Specifically, AVC is not visualized in the A4c-view (inferoseptum), while the AK-wave propagate out of the PLAX-view to reach the basal anteroseptum. Variation was minimized by using a standardized protocol and averaging the MWV over 2-4 cardiac cycles. Discrepancy in each manual step, such as event timing, M-mode line placement, and MWV measurement may cause variation. M-mode line placement in the B-mode image is probably the most critical, as minor alterations affect the MWV estimates. Additionally, optimal recordings of standard views should be targeted.

#### MWV in AS

In AS patients, we observed lower feasibility in 3 of 6 combinations of walls and events, with the inferoseptal (not for AVC) and inferolateral walls having similar feasibility to healthy subjects (Table 5A). There was a trend towards higher average MWV in patients with AS for all LV walls, though only significant for the 2 septal walls after AVC (Table 5B and Figure 3). This contrasts to 2 previous studies reporting higher AK-MWVs in patients with AS compared with healthy subjects (7,11). In both these studies more recordings were feasible for MWV analysis in patients. Furthermore, the estimated MWVs were based on the average of 6 apical walls with a lower frame rate, and 3D-recordings respectively, meaning that results are not directly comparable. The Pislaru-group found even larger difference between amyloidosis patients and healthy subjects compared with the difference from healthy subjects to AS patients (11,16). Furthermore, and supporting previous studies, the variation of MWVs was larger among patients compared with healthy subjects across walls (Table 7) (5-7,11,13-16,18). Limited correlation with CMR results and limited correlation for the AK MWV combined with higher AVC MWV,

indicate that differences in load and contractile state may explain the higher MWVs in patients, possibly indicating a struggling myocardium.

Compared with healthy subjects patients with severe AS demonstrated larger and less compliant left atria (lower reservoir strain and lower a') and a larger delay from the start of the septal a' to the start of the septal propagation of the AK-wave, possibly affecting the AK-wave. The AK-wave should be further studied experimentally and clinically to improve the understanding of diastolic function and atrioventricular interaction.

#### Comparisons to clinical and imaging parameters

We found no systematic correlation between MWVs and standard imaging parameters.

Measurement errors and waves travelling out of plane may partly explain these results. We observed a weak positive association between quantitative CMR measures and anteroseptal MWV after AVC (Figure 4). This weak relation indicates that MWVs provide additional information on myocardial stiffness compared with CMR and is not merely a surrogate marker for fibrosis. Furthermore, this study is not powered to investigate the relation between MWVs and other imaging parameters indicating myocardial fibrosis (5,15,16).

#### MWV in HUNT-4

These healthy subjects were comparable to Population-StOlav, but somewhat younger and healthier. Compared with the septum, a higher AK-MWV in the lateral wall was confirmed in Population-HUNT. Additionally, a lower inferoseptal AVC-MWV was reproduced among healthy subjects compared with patients. Population-HUNT consisted of more females, were younger and with higher frame rates obtained than in Population-StOlav. They did not undergo CMR or parasternal HFR-recordings, and most MWVs were measured only once (Table 1).

Single MWV measurement might limit the robustness and reduced feasibility for the MWV estimates, compared with Population-StOlav (Table 5A). Nevertheless, finding similar MWVs across waves and triggering events, as in healthy subjects from Population-StOlav, is reassuring (Table 5B).

### Limitations

As discussed above, the two populations did not undergo identical examinations (Table 1). The fixed image sector resulted in incomplete imaging of the inferolateral wall in 2 cases in Population-StOlav. Higher frame rate particularly limits lateral resolution and image contrast, possibly affecting both acquisition and analysis. Individual wall scanning would provide higher temporal resolution with preserved spatial resolution but may increase load variation between scans. MWVs depend on geometry, load, and the stiffness of the medium the wave propagates through. For an elastic, isotropic and homogenous bulk material, the shear wave velocity is proportional to the stiffness of the material (4,14,29,32). Due to long wavelengths, the complex boundary conditions affecting the mechanical wave propagation and unfulfilled physical assumptions for the myocardium, we refrained from computing stiffness. Instead, we have presented the MWVs known to correlate to myocardial stiffness (3,14,26,29,32). Furthermore, we used identical smoothing parameters for both AK and AVC wave to simplify the analysis procedure. However, as these waves have different wave propagation patterns and dispersion behavior, it would have been more precise to use smoothing parameters adapted to each wave.

### Conclusions

Mechanical wave imaging is a promising method for evaluation of myocardial stiffness. Using a clinical ultrasound scanner, detection of AK-waves is highly feasible. We present indicators for mechanical wave quality assessment and advocate the use of such for improved consistency. The

AK lateral MWVs were higher than septal MWVs. Moreover, similar MWVs were observed in two healthy populations. Patients with AS demonstrated clearly higher MWVs at AVC, compared with healthy subjects, illustrating that differences in load and contractile state affects the MWV. Larger studies on patients with varying degrees of AS is needed to clarify the role of this technique in the follow up of patients with AS.



## Perspectives

### Clinical competencies

HFR imaging with the visualization of myocardial mechanical waves provides a new approach to evaluation of myocardial stiffness. HFR echocardiography may add information to CMR for evaluating myocardial stiffness, and could ultimately improve management of cardiac disease (3). This study provides new insights in evaluating MWV and supports previous studies demonstrating that AVC-MWVs separate cardiac patients from healthy subjects.

### Translational outlook

Automatization of the MWV-analysis will further improve precision and reduce measurement errors (26,27). With the ongoing technical development of ultrasound scanners and probes, higher temporal and spatial resolution is achievable, possibly making this method even more applicable for routine clinical work. Imaging four LV walls provides information about myocardial stiffness from large parts of the LV. Furthermore, 3D imaging may overcome challenges due to complex LV geometry and out of plane wave propagation, and hence could provide regional and global measures of myocardial stiffness from a single acquisition (3,7,8).

## References

1. Espeland T, Lunde IG, Amundsen BH, Gullestad L, Aakhus S. Myocardial fibrosis. *Tidsskr Nor Laegeforen* 2018;138.
2. Karamitsos TD, Arvanitaki A, Karvounis H, Neubauer S, Ferreira VM. Myocardial Tissue Characterization and Fibrosis by Imaging. *J Am Coll Cardiol Img* 2020;13:1221-1234.
3. Villemain O, Baranger J, Friedberg MK et al. Ultrafast Ultrasound Imaging in Pediatric and Adult Cardiology: Techniques, Applications, and Perspectives. *J Am Coll Cardiol Img* 2020;13:1771-1791.
4. Strachinaru M, Bosch JG, van Dalen BM et al. Cardiac Shear Wave Elastography Using a Clinical Ultrasound System. *Ultrasound Med Biol* 2017;43:1596-1606.
5. Strachinaru M, Bosch JG, van Gils L et al. Naturally Occurring Shear Waves in Healthy Volunteers and Hypertrophic Cardiomyopathy Patients. *Ultrasound Med Biol* 2019;45:1977-1986.
6. Strachinaru M, Geleijnse ML, de Jong N et al. Myocardial Stretch Post-atrial Contraction in Healthy Volunteers and Hypertrophic Cardiomyopathy Patients. *Ultrasound Med Biol* 2019;45:1987-1998.
7. Salles S, Espeland T, Molares A et al. 3D Myocardial Mechanical Wave Measurements: Toward In Vivo 3D Myocardial Elasticity Mapping. *J Am Coll Cardiol Img* 2021;14:1495-1505.
8. Pernot M, Couade M, Mateo P, Crozatier B, Fischmeister R, Tanter M. Real-time assessment of myocardial contractility using shear wave imaging. *J Am Coll Cardiol* 2011;58:65-72.
9. Villemain O, Correia M, Mousseaux E et al. Myocardial Stiffness Evaluation Using Noninvasive Shear Wave Imaging in Healthy and Hypertrophic Cardiomyopathic Adults. *J Am Coll Cardiol Img* 2019;12:1135-1145.
10. Pislaru C, Pellikka PA, Pislaru SV. Wave propagation of myocardial stretch: correlation with myocardial stiffness. *Basic Res Cardiol* 2014;109:438.

11. Pislaru C, Alashry MM, Thaden JJ, Pellikka PA, Enriquez-Sarano M, Pislaru SV. Intrinsic Wave Propagation of Myocardial Stretch, A New Tool to Evaluate Myocardial Stiffness: A Pilot Study in Patients with Aortic Stenosis and Mitral Regurgitation. *J Am Soc Echocardiogr* 2017;30:1070-1080.
12. Pernot M, Lee WN, Bel A et al. Shear Wave Imaging of Passive Diastolic Myocardial Stiffness: Stunned Versus Infarcted Myocardium. *J Am Coll Cardiol Img* 2016;9:1023-1030.
13. Cvijic M, Bézy S, Petrescu A et al. Interplay of cardiac remodelling and myocardial stiffness in hypertensive heart disease: a shear wave imaging study using high-frame rate echocardiography. *Eur Heart J Cardiovasc Imaging* 2020;21:664-672.
14. Petrescu A, Santos P, Orłowska M et al. Velocities of Naturally Occurring Myocardial Shear Waves Increase With Age and in Cardiac Amyloidosis. *J Am Coll Cardiol Img* 2019;12:2389-2398.
15. Petrescu A, Bézy S, Cvijic M et al. Shear Wave Elastography Using High-Frame-Rate Imaging in the Follow-Up of Heart Transplantation Recipients. *J Am Coll Cardiol Img* 2020;13:2304-2313.
16. Pislaru C, Ionescu F, Alashry M et al. Myocardial Stiffness by Intrinsic Cardiac Elastography in Patients with Amyloidosis: Comparison with Chamber Stiffness and Global Longitudinal Strain. *J Am Soc Echocardiogr* 2019;32:958-968.e4.
17. Kvåle KF, Salles S, Lervik LCN et al. Detection of Tissue Fibrosis using Natural Mechanical Wave Velocity Estimation: Feasibility Study. *Ultrasound Med Biol* 2020;46:2481-2492.
18. De Jesus T, Alashry MM, Padang R et al. Intrinsic cardiac elastography in patients with primary mitral regurgitation: predictive role after mitral valve repair. *Eur Heart J Cardiovasc Imaging* 2020.
19. Salles S, Lovstakken L, Aase SA, Bjastad TG, Torp H. Clutter Filter Wave Imaging. *IEEE Trans Ultrason Ferroelectr Freq Control* 2019;66:1444-1452.

20. Eriksen-Volnes T GJ, Olaisen SH, Letnes JM, Nes B, Lovstakken L, Wisløff U, Dalen, H. Updated Normalized Values From Guideline-Directed Dedicated Views for Cardiac Dimensions and Left Ventricular Diastolic and Systolic Function in a Healthy Population - Data From the HUNT4Echo Study. *J Am Coll Cardiol Img* 2023.
21. Lang RM, Badano LP, Mor-Avi V et al. Recommendations for cardiac chamber quantification by echocardiography in adults: an update from the American Society of Echocardiography and the European Association of Cardiovascular Imaging. *Eur Heart J Cardiovasc Imaging* 2015;16:233-70.
22. Nagueh SF, Smiseth OA, Appleton CP et al. Recommendations for the Evaluation of Left Ventricular Diastolic Function by Echocardiography: An Update from the American Society of Echocardiography and the European Association of Cardiovascular Imaging. *Eur Heart J Cardiovasc Imaging* 2016;17:1321-1360.
23. Messroghli DR, Moon JC, Ferreira VM et al. Clinical recommendations for cardiovascular magnetic resonance mapping of T1, T2, T2\* and extracellular volume: A consensus statement by the Society for Cardiovascular Magnetic Resonance (SCMR) endorsed by the European Association for Cardiovascular Imaging (EACVI). *J Cardiovasc Magn Reson* 2017;19:75.
24. Schulz-Menger J, Bluemke DA, Bremerich J et al. Standardized image interpretation and post-processing in cardiovascular magnetic resonance - 2020 update : Society for Cardiovascular Magnetic Resonance (SCMR): Board of Trustees Task Force on Standardized Post-Processing. *J Cardiovasc Magn Reson* 2020;22:19.
25. Heiberg E, Sjögren J, Ugander M, Carlsson M, Engblom H, Arheden H. Design and validation of Segment--freely available software for cardiovascular image analysis. *BMC Med Imaging* 2010;10:1.

26. Santos P, Petrescu AM, Pedrosa JP et al. Natural Shear Wave Imaging in the Human Heart: Normal Values, Feasibility, and Reproducibility. *IEEE Trans Ultrason Ferroelectr Freq Control* 2019;66:442-452.
27. Keijzer LBH, Strachinaru M, Bowen DJ et al. Reproducibility of Natural Shear Wave Elastography Measurements. *Ultrasound Med Biol* 2019;45:3172-3185.
28. Brekke B, Nilsen LC, Lund J et al. Ultra-high frame rate tissue Doppler imaging. *Ultrasound Med Biol* 2014;40:222-31.
29. Keijzer LBH, Strachinaru M, Bowen DJ et al. Parasternal Versus Apical View in Cardiac Natural Mechanical Wave Speed Measurements. *IEEE Trans Ultrason Ferroelectr Freq Control* 2020;67:1590-1602.
30. Strachinaru M, Bosch JG, Schinkel AFL et al. Local myocardial stiffness variations identified by high frame rate shear wave echocardiography. *Cardiovasc Ultrasound* 2020;18:40.
31. Voigt JU, Lindenmeier G, Werner D et al. Strain rate imaging for the assessment of preload-dependent changes in regional left ventricular diastolic longitudinal function. *J Am Soc Echocardiogr* 2002;15:13-9.
32. Voigt JU. Echocardiographic Stiffness Measurements: How to Rule the Waves? *J Am Coll Cardiol Img* 2021;14:1506-1507.

Figures

Central Illustration

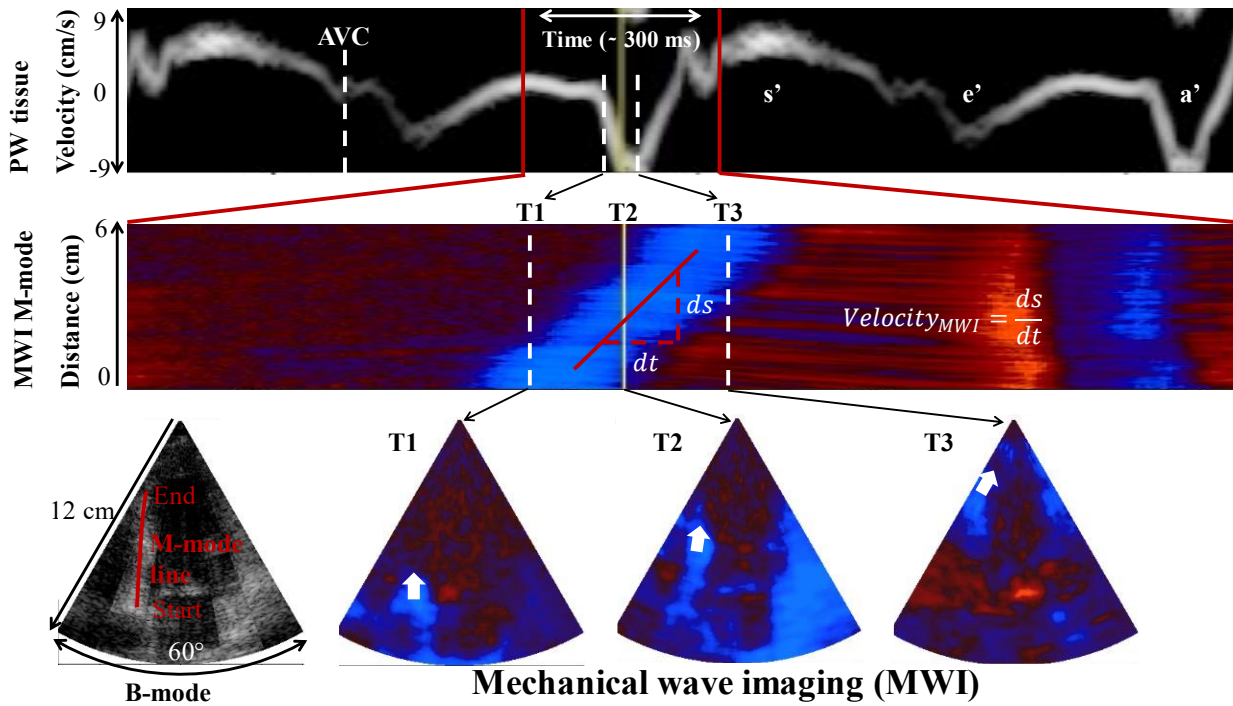
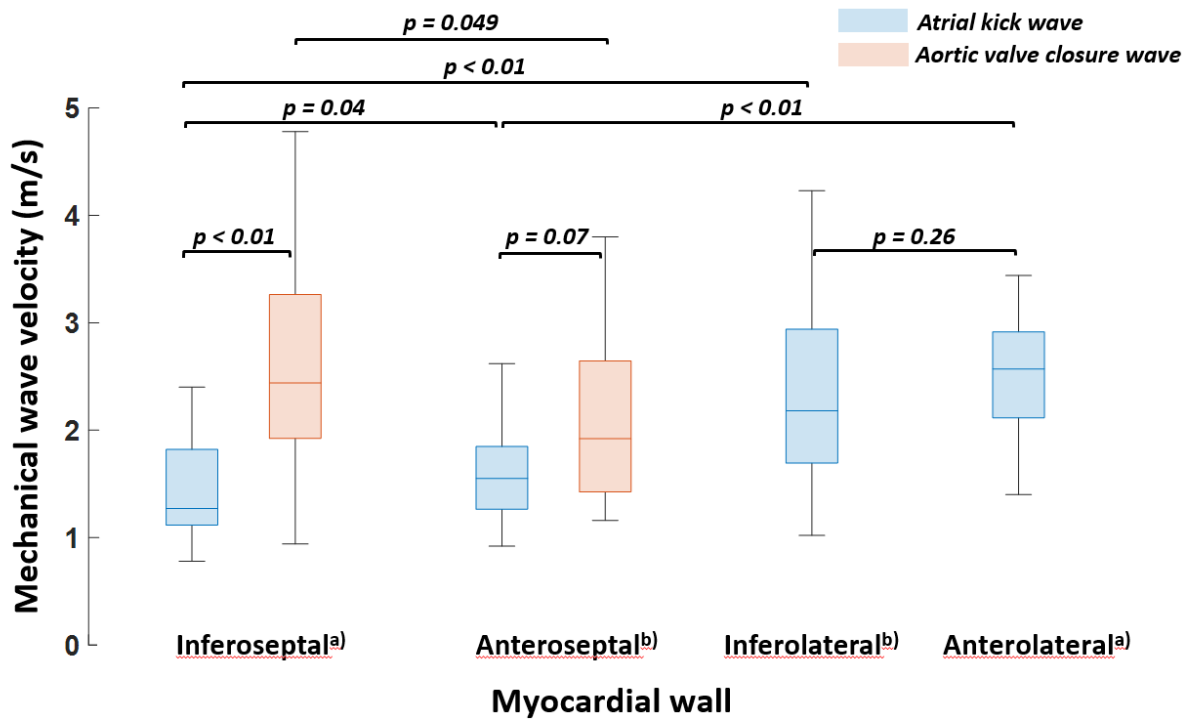
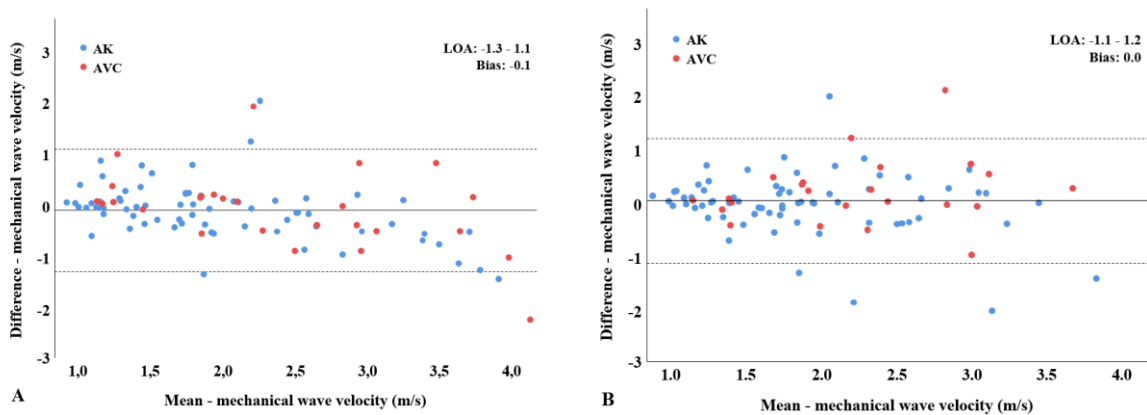


Figure 1.



**Figure 2.**



**Figure 3.**

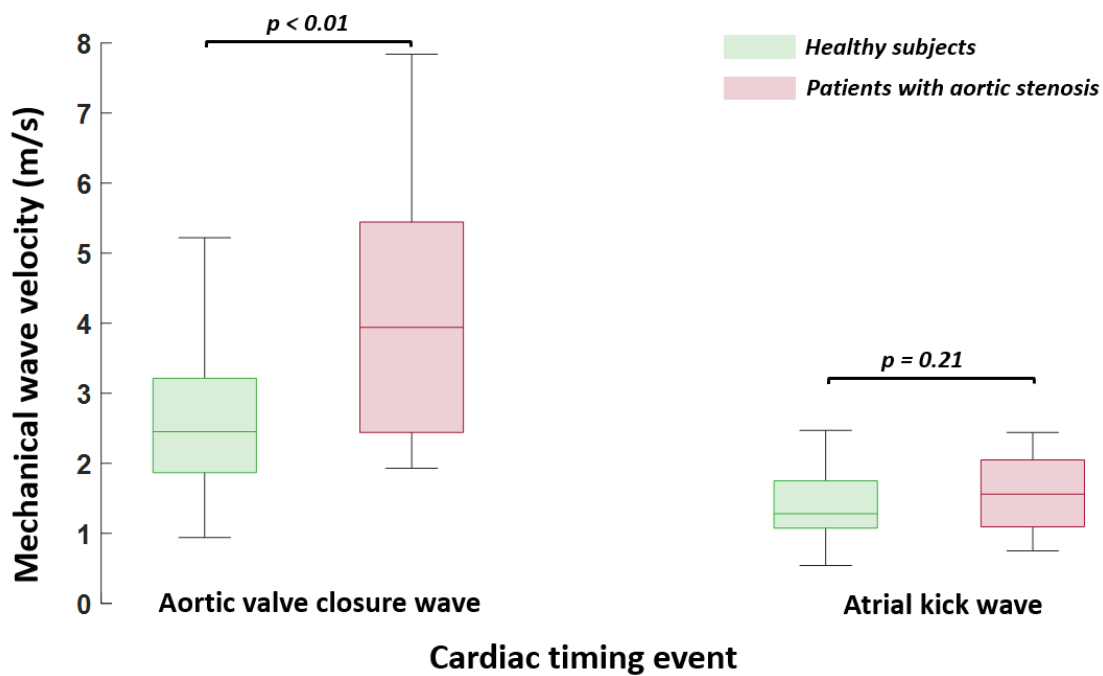
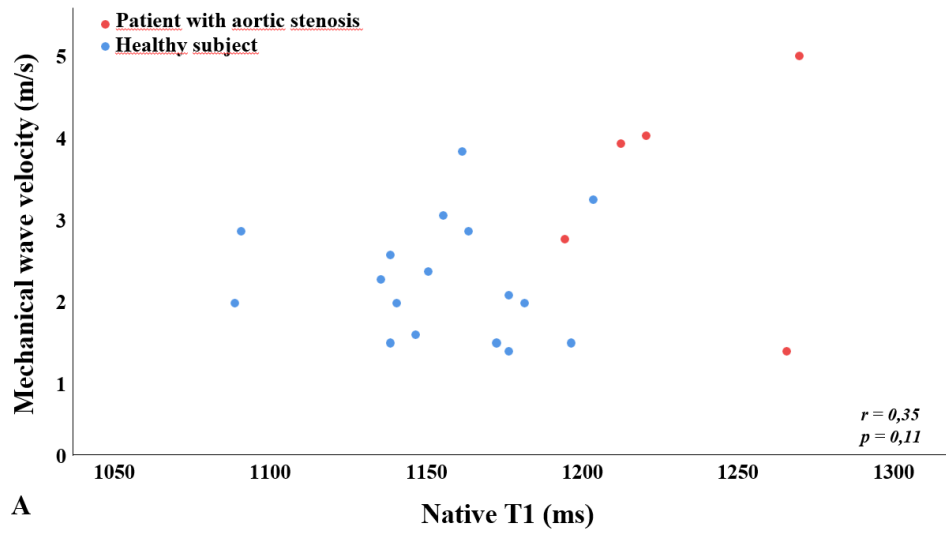
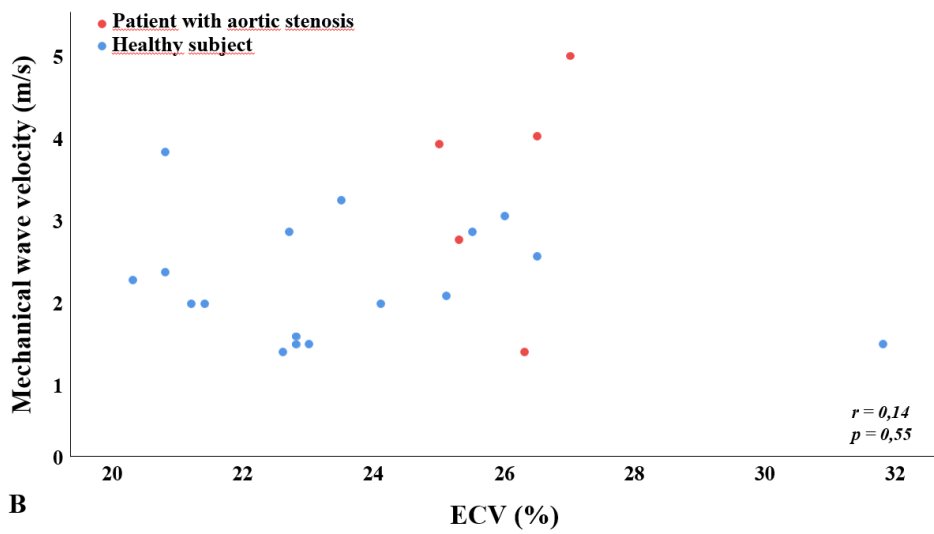


Figure 4.



A



B



## Figure titles and legends

### **Central Illustration. Mechanical wave imaging**

Two cardiac cycles are covered. The Doppler spectrum (PW-tissue) is used for timing. Systolic shortening (s') and early (e') and late (a') diastolic lengthening and aortic valve closure (AVC) are marked in the figure. The M-mode line is placed in the apical 4-chamber B-mode image (bottom left). The atrial kick wave is propagating in the inferoseptum, from base (T1) - midventricular part (T2) - apex (T3) (blue wavefront). The mechanical wave velocity is the slope of the M-mode line (ds/dt).

### **Figure 1. Mechanical wave velocities in healthy subjects**

Box plot depicting mechanical wave velocities (MWVs) in healthy subjects from Population-StOlav at the atrial kick (AK) and aortic valve closure (AVC) for the four left ventricular walls covered by the A4c (a) and PLAX-view (b). The central box represents the 25-75-percentile of values, the middle line the median, and the line extends from minimum - maximum value. MWVs from different walls and events are compared, and relevant p-values are reported.

### **Figure 2. Reproducibility for mechanical wave velocities in healthy subjects**

Bland Altman plots for the intraobserver (A) and interobserver (B) variability of mechanical wave velocities for left ventricular walls and two cardiac cycle events. Limit of agreement (LOA) is defined as  $\text{bias} \pm 1.96 \times \text{SD}$ . The dashed lines represent the upper and lower LOA, while the solid line represents bias.

### **Figure 3. Mechanical wave velocities in healthy subjects and severe aortic stenosis**

Box plot depicting inferoseptal (PLAX-view) mechanical wave velocities (MWVs) at atrial kick and aortic valve closure and comparing MWVs between patients and two healthy populations.

#### **Figure 4. Mechanical wave velocities in relation to CMR parameters**

Scatter plots illustrating a weak positive correlation between antero-septal (PLAX-view) wave velocities after aortic valve closure and native T1 (A) and extracellular volume (ECV) (B). The presumed healthy outlier in B was an octogenarian later diagnosed with AL amyloidosis, possibly indicating that the increased ECV was a marker of subclinical structural cardiac disease. If removed, correlation would approach significance ( $r=0,38,p=0.09$ ).

## Tables

**Table 1. Overview of the different populations in this study**

	Population		
	Healthy (HS) <sup>a)</sup>	HUNT-4 (HH)	Patients (P) <sup>a)</sup>
Subjects (N)	29	34	13
Views covered <sup>b)</sup>	PLAX and A4C	A4C	PLAX and A4C
CMR performed	+	-	+
Cardiac cycles per view (mode) (N)	3	1	3
Frame rate (/s)	858 ± 0	1403 (1213–1619)	858 ± 0

Values are mean ± SD, median (interquartile range) or n (%).

A4C = Apical 4 chamber; CMR = Cardiac magnetic resonance imaging; HH = Healthy

Population-HUNT; HS = Healthy Population StOlav; P = Patients with aortic stenosis; PLAX =

Parasternal long axis

- a) Healthy population StOlav (HS) and patients (P) were both included at St. Olavs hospital and together constitute the Population-StOlav.
- b) The PLAX-view covers the anteroseptal and inferolateral wall. The A4C-view covers the inferoseptal and anterolateral wall.

**Table 2. Population characteristics and laboratory results**

	Population			P-value		
	Healthy (HS) (N = 29)	HUNT-4 (HH) (N = 34)	Patients (P) (N = 13)	HS-HH	HS-P	HH-P
Age, years	69 ± 10	64 ± 11	69 ± 12	0.036	0.940	0.132
Males, N (%)	18 (62 %)	14 (41 %)	8 (62 %)	0.131	1.000	0.328
SBP, mm Hg	137 ± 20	135 ± 22	135 ± 17	0.674	0.824	0.899
DBP, mm Hg	79 ± 7	78 ± 11	76 ± 5	0.606	0.227	0.671
Heart rate, beats/min	63 ± 9	66 ± 9	64 ± 9	0.198	0.734	0.492
Smokers, N (%)	2 (7 %)	1 (3 %)	1 (8 %)	0.590	1.000	0.481
DM II, N (%)	2 (7 %)	0 (0 %)	0 (0 %)	0.208	1.000	-
Hypertension, N (%)	2 (7 %)	0 (0 %)	4 (31 %)	0.208	0.063	0.004
BMI, kg/m <sup>2</sup>	26 ± 3	25 ± 3	26 ± 5	0.399	0.891	.443
<b>Lab-results</b>						
HbA1c, mmol/mol	37 (34 - 39)	35 (32 - 37)	35 (33 - 38)	0.012	0.260	0.444
Hemoglobin, g/dl	13.8 ± 1.1	14.9 ± 1.0	14.2 ± 1.1	<0.001	0.303	0.054
CRP, mg/l	0.8 (0.4 - 1.4)	0.9 (0.5 - 1.5)	1.1 (0.7 - 4.5)	0.468	0.090	0.040
Creatinine, µmol/l	71 (64 - 77)	73 (67 - 84)	72 (61 - 90)	0.324	0.456	0.498
NT-proBNP, ng/l	48 (30 - 99)		378 (171 - 1142)		<0.001	
Troponine T, ng/l	<10 (<10 - 11)		15 (<10 - 18)		0.102	

Values are mean ± SD, median (interquartile range) or n (%).

BMI = body mass index; CRP = c-reactive protein; DBP = diastolic blood pressure; DM2= diabetes mellitus type 2; HbA1c = hemoglobin A1c; HH = Healthy Population-HUNT; HS = Healthy Population StOlav; NT-proBNP = n-terminal prohormone of brain natriuretic peptide; P = Patients with aortic stenosis; SBP = systolic blood pressure; Smokers = current smokers.

**Table 3. Findings from cardiac imaging in different populations**

	Population			P-value		
	Healthy (HS) (N = 29)	HUNT-4 (HH) (N = 34)	Patients (P) (N = 13)	HS-HH	HS-P	HH-P
AV peak velocity, m/s	1.3 ± 0.2	1.4 ± 0.2	5.3 ± 0.9	0.020	<0.001	<0.001
<b><u>LV dimensions</u></b>						
IVSd, mm	10 ± 2	9 ± 2	15 ± 2	<0.001	<0.001	<0.001
LVIDd, mm	48 ± 4	48 ± 6	45 ± 4	0.738	<0.001	0.077
PWTd, mm	7 (6 - 8)	7 (7 - 9)	10 (10 - 11)	0.047	<0.001	<0.001
Mass <sub>i</sub> , g/m <sup>2</sup> (2D)	74 ± 15	69 ± 19	115 ± 26	0.238	<0.001	<0.001
Mass <sub>i</sub> , g/m <sup>2</sup> (CMR)	69 ± 14		91 ± 20		<0.001	
EDV <sub>i</sub> , ml/m <sup>2</sup> (2D)	67 ± 15	53 ± 10	75 ± 16	<0.001	0.151	<0.001
EDV <sub>i</sub> , ml/m <sup>2</sup> (3D)	72 ± 13	56 ± 10	83 ± 13	<0.001	0.015	<0.001
EDV <sub>i</sub> , ml/m <sup>2</sup> (CMR)	78 ± 13		79 ± 12		0.810	
<b><u>LV systolic function</u></b>						
MAPSE average, mm	13 ± 2		11 ± 2		<0.001	
S' average, cm/s	7 (7 - 9)	7 (7 - 9)	6 (5 - 7)	0.976	<0.001	<0.001
GLS, %	-18 ± 2	-20 ± 2	-15 ± 2	0.012	<0.001	<0.001
EF, % (2D)	57 ± 4	60 ± 4	55 ± 6	0.013	0.205	<0.001
EF, % (3D)	56 ± 4	60 ± 4	52 ± 7	<0.001	0.020	<0.001
EF, % (CMR)	61 ± 5		67 ± 9		0.006	
Mech. disp., ms	52 ± 11		62 ± 12		0.014	
<b><u>LV diastolic function</u></b>						
E' average, cm/s	7 (6 - 8)	8 (6 - 10)	6 (4 - 6)	0.110	0.005	0.001
A' average, cm/s	9 (8 - 11)	10 (9 - 11)	8 (7 - 9)	0.322	0.006	<0.001
MV DT, ms	189 (152 - 239)	200 (181 - 228)	220 (181 - 260)	0.129	0.151	0.373
MV E/A-ratio	1.0 (0.8 - 1.1)	0.9 (0.7 - 1.1)	0.9 (0.7 - 1.1)	0.634	0.727	0.961
E/E'-ratio	8 (6 - 10)	8 (6 - 9)	12 (12 - 18)	0.784	<0.001	<0.001
TR V-max, m/s	2.2 ± 0.2	2.1 ± 0.3	2.6 ± 0.4	0.253	<0.001	<0.001
LAV <sub>i</sub> , ml/m <sup>2</sup> (2D)	36 ± 10	31 ± 12	49 ± 10	0.078	0.001	<0.001
LAV <sub>i</sub> , ml/m <sup>2</sup> (3D)	37 ± 9	31 ± 8	47 ± 11	0.006	0.007	<0.001
LA Res. strain, %	27 ± 5	30 ± 7	18 ± 6	0.118	<0.001	<0.001
<b><u>CMR – tissue characteristics</u></b>						
Native T1, ms	1158 (1140 - 1184)		1213 (1175 - 1268)		<0.001	
ECV, %	24 ± 3		25 ± 2		0.205	

Values are mean ± SD or median (interquartile range).

A' = peak late diastolic annular plane velocity; AV peak velocity = antegrade peak velocity across the aortic valve; DT = deceleration time of transmitral E-wave; E' = peak early diastolic annular plane velocity; E/E' = relation between early transmitral velocity and E'; E/A = relationship between early and late diastolic transmitral velocity; ECV = extracellular volume; EDVi = end diastolic volume indexed to body surface area; EF = ejection fraction; GLS = global longitudinal strain; HH = Healthy Population-HUNT; HS = Healthy Population StOlav; IVSd = end diastolic thickness of intraventricular septum; LVIDd = end diastolic dimension of LV-cavity; LA Res. strain = left atrial reservoir strain. LAVi = left atrial volume at end systole, indexed to body surface area; LV = left ventricle; MAPSE = mitral annular plane systolic excursion; Mass<sub>i</sub> = mass indexed to body surface area; Mech. disp. = standard deviation of time to peak negative strain in all LV-segments; MV = Mitral valve; P = Patients with aortic stenosis; PWTd = end diastolic thickness of posterior wall; S' = peak systolic annular plane velocity; TR V-max = tricuspid regurgitation, peak jet velocity.

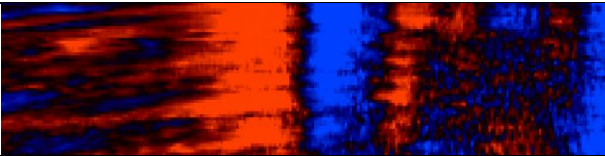
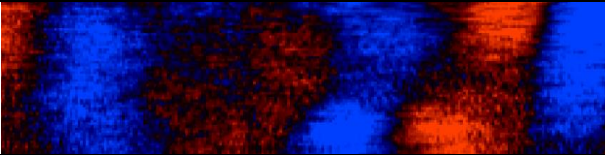
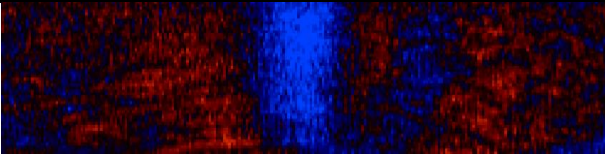
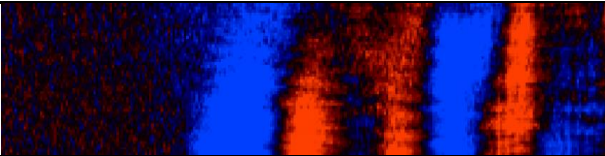
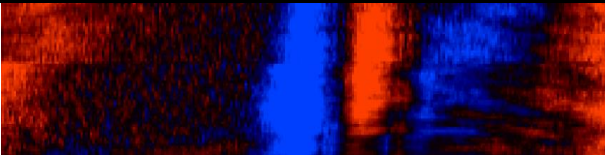
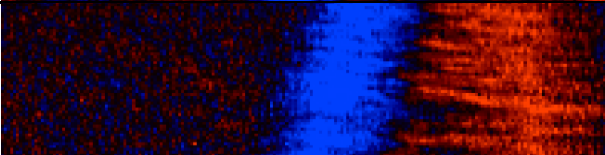
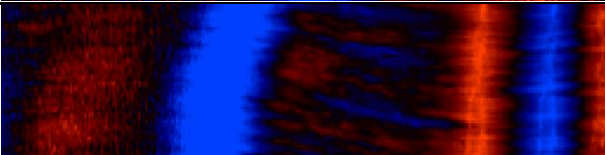
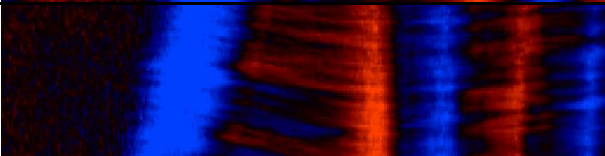
Rating	Meaning	Illustration	Wave count (%)		
			HS (N = 29)	HH (N = 34)	P (N = 13)
1	Unphysiological MWV (AVC >9.0 m/s or AK >7.0 m/s)		16 (3.0%)	23 (11,2 %)	12 (5,4 %)
2	Bidirectional wave propagation		28 (5.3%)	23 (11,2 %)	30 (13,5 %)
3	Poor image quality		38 (7.1%)	26 (12,7 %)	26 (11,7 %)
4	Wave appears broader in one end		150 (28,2 %)	107 (52,2 %)	94 (42,2 %)
5	Significant horizontal stitching artefact		12 (2,3 %)	0 (0 %)	2 (0,9 %)
6	Clear direction of the wave, medium broad		230 (43,2 %)	22 (10,7 %)	38 (17,0 %)
7	Wave with non-linear velocities, notch		30 (5,6 %)	4 (2,0 %)	19 (8,5 %)
8	Linear and narrow wave, considered optimal		28 (5,3 %)	0 (0 %)	2 (0,9 %)
Total	Discarded waves		82 (15,4 %)	72 (35,1 %)	68 (30,5 %)
	Accepted waves		450 (84,6 %)	133 (64,9 %)	155 (69,5 %)
	Total waves		532 (100 %)	205 (100 %)	223 (100 %)

Table 4. Systematic evaluation of mechanical wave quality in healthy subjects

Systematic evaluation of mechanical wave quality according to our criteria in healthy subjects from Population-HUNT and Population-StOlav, and in patients with aortic stenosis.

Ratings marked in red (1-3) led to rejection of the wave, while waves rated 4-8 (green) was included for further analysis.

AK = Atrial kick; AVC = Aortic valve closure; HH = Healthy Population-HUNT; HS = Healthy Population StOlav; MWV = Mechanical wave velocity; P = Patients with aortic stenosis.



**Table 5.**

**A. Feasibility and quality assessment for mechanical waves in healthy subjects and patients with aortic stenosis**

Event	Wall	Subject	Valid <sup>a)</sup> measurements (%)	Subjects with $\geq 50\%$ valid measurements (%)	Length, mm <sup>b)</sup>
AK	Inferolateral	HS	80 / 86 (93)	27 (93)	30 $\pm$ 8
		P	37 / 39 (95)	13 (100)	24 $\pm$ 6
AK	Anterolateral	HS	86 / 91 (95)	28 (97)	40 $\pm$ 9
		HH	21 / 29 (72)	19 (73)	38 $\pm$ 7
		P	21 / 35 (60)	8 (67)	38 $\pm$ 5
AK	Anteroseptum	HS	80 / 86 (93)	27 (93)	28 $\pm$ 6
		P	28 / 39 (72)	10 (77)	23 $\pm$ 6
AK	Inferoseptum	HS	93 / 93 (100)	29 (100)	37 $\pm$ 8
		HH	27 / 32 (84)	26 (93)	30 $\pm$ 7
		P	40 / 42 (95)	12 (92)	32 $\pm$ 7
AVC	Anteroseptum	HS	59 / 88 (67)	20 (69)	22 $\pm$ 3
		P	13 / 36 (36)	5 (38)	20 $\pm$ 5
AVC	Inferoseptum	HS	52 / 88 (59)	19 (66)	25 $\pm$ 6
		HH	15 / 33 (45)	14 (45)	22 $\pm$ 8
		P	20 / 38 (53)	8 (62)	26 $\pm$ 6

**B. Mechanical wave velocities in healthy subjects and patients with aortic stenosis**

Event	Wall	Mechanical wave velocity (m/s)			P-value		
		Healthy (HS)	HUNT-4 (HH)	Patients (P)	HS-HH	HS-P	HH-P
AK	Inferolateral	2.3 $\pm$ 0.8		2.6 $\pm$ 0.9			0.287
AK	Anterolateral	2,6 (2,1 - 2,9)	3,0 (2,6 - 3,6)	2,9 (2,2 - 4,5)	0.020	0.320	1.000
AK	Anteroseptum	1.6 (1.3 - 1.9)		1.7 (1.3 - 2.7)			0.511
AK	Inferoseptum	1.3 (1.1 - 1.8)	1,3 (1,0 - 1,7)	1.4 (1.1 - 2.1)	0.522	0.372	0.256
AK	Average <sup>c)</sup>	2.0 $\pm$ 0.3		2.2 $\pm$ 0.6			0.107
AVC	Anteroseptum	2.1 $\pm$ 0.7		3.4 $\pm$ 1.4			0.007
AVC	Inferoseptum	2.6 $\pm$ 0.9	2,6 $\pm$ 1.1	4.2 $\pm$ 2.1	0.944	0.009	0.030

Feasibility and quality assessment of mechanical waves and estimation of mechanical wave velocities at different events in left ventricular walls in Healthy Population HUNT (N = 34), Healthy Population StOlav (N = 29) and Patients (N = 13).

Values are mean  $\pm$  SD, median (interquartile range) or n (%).

AK = Atrial kick; AVC = Aortic valve closure; HH = Healthy Population HUNT; HS = Healthy Population StOlav; P = Patients with aortic stenosis

- a) Accepted measurements divided by total number of measurements. All individuals, except Population-HUNT had 2 – 4 measurements of wave velocities for a given wall and event.
- b) Length of traced M-mode line
- c) Average value of atrial kick mechanical wave velocities for subjects with valid registrations from at least  $\frac{3}{4}$  walls, all healthy subjects from Population-StOlav and 12/13 patients were included.

**Table 6. Agreement analysis among healthy subjects from Population StOlav**

Event	Wall	No. of comparisons		LOA		ICC	
		Intra-observer	Inter-observer	Intraobserver (m/s)	Interobserver (m/s)	Intraobserver	Interobserver
AK	Inferolateral	17	17	-1.5 - 0.8	-1.4 - 1.0	0.83 (0.47-0.94)	0.78 (0.42-0.92)
AK	Anterolateral	19	19	-1.2 - 0.8	-1.6 - 1.4	0.88 (0.69-0.95)	0.60 (-0.06-0.85)
AK	Anteroseptum	17	13	-1.3 - 1.5	-1.1 - 1.4	0.72 (0.22 - 0.90)	-0.28 (-3.37-0.62) a)
AK	Inferoseptum	20	20	-0.6 - 0.5	-0.4 - 0.4	0.89 (0.72-0.96)	0.95 (0.88-0.98)
AVC	Anteroseptum	14	10	-1.8 - 2.2	-0.9 - 1.1	0.87 (0.59-0.96)	0.92 (0.66-0.98)
AVC	Inferoseptum	12	13	-1.9 - 1.6	-1.1 - 1.7	0.71 (-0.02-0.92)	0.42 (-0.70-0.82)
AK	All 4 walls	73	69	-1.2 - 1.0	-1.2 - 1.1	0.88 (0.80 - 0.92)	0.82 (0.71 - 0.89)
AVC	2 septal walls	26	23	-1.6 - 1.5	-1.0 - 1.4	0.82 (0.60 - 0.92)	0.78 (0.49 - 0.91)
Both	All walls	99	92	-1.3 - 1.1	-1.1 - 1.2	0.86 (0.80 - 0.91)	0.82 (0.72 - 0.88)

LOA and ICC for different events across different myocardial walls in healthy subjects from

Population-StOlav (N = 29). LOA are given as ranges in mechanical wave velocities (m/s); bias

$\pm 1.96 \times SD$ . ICC, using the two-way mixed model, with average measures and absolute

agreement, are presented as mean (95 % confidence interval).

AK = Atrial kick; AVC = Aortic valve closure; ICC = Intraclass correlation coefficient; LOA =

Limits of agreement

a) If the major outlier was excluded, this interobserver ICC would be 0,51 (-0,92-0,86).

**Table 7. Overview of previous studies reporting natural mechanical wave velocities<sup>a)</sup>**

Study, year, (ref)	View	Wall	Method	Scanner	FPS	Population	N	Age	Mechanical wave velocity (m/s) - event		
									AVC	MVC	AK
Voigt, 2002 (31)	Apical	6 walls, mean	TVI/SRI	GEVU, system five	178	Healthy	20	24			2.0±0.1
Brekke, 2014 (28)	A4C	Inferoseptum	TDI	GEVU, E9	1200	Healthy	10	25-43	5.4±1.3		
Pislaru, 2014 (10)	Apical	6 walls, mean	TDI	GEVU, E9	350 - 450	Healthy	10	52±16			1.4±0.2
Pislaru, 2017 (11)	Apical	6 walls, mean	TDI	GEVU, E9 or vivid Q	350 - 460	Severe aortic stenosis Severe mitral regurg.	20	58±14 73±11			1.4±0.2 2.2±0.7
Pislaru, 2019 (16)	Apical	6 walls, mean	TDI	GEVU, E9 or E95	250 - 465	Health volunteers Cardiac amyloidosis Non cardiac amyloidosis	40	64±10 66±9 49±13			1.6±0.2 3.2±1.0 1.8±0.4
Santos, 2019 (26)	PLAX	Anteroseptum	TDI	HD-PULSE	1066±160	Healthy	30	31±5	3.5±0.6		3.2±0.6
Petrescu, 2019 (14)	PLAX	Anteroseptum	TDI	HD-PULSE	1150±245	Healthy	46	44±17	3.8±0.8		3.5±0.9
Cvijic, 2019 (13)	PLAX	Anteroseptum	TDI	HD-PULSE	1266±317	Cardiac amyloidosis Hypertension	17	68±10 26 55±15 59±14	5.6±1.1		6.3±1.6 4.0±1.0 5.8±1.2
Strachinaru, 2019 (5)	PLAX	Anteroseptum	TDI	Philips IE33	516±13 519±18	Healthy HCM	45 43	34±13 51±12	3.6±0.5 5.1±0.7		4.7±0.8 6.9±1.2
Strachinaru, 2019 (6)	A4C	Inferoseptum	TDI	Philips IE33	542±30 530±20	Healthy HCM	42 33	35±14 49±13			1.6±0.3 1.8±0.8
Keijzer, 2019 (27)	PLAX	Anteroseptum	TDI	Zonare Z53 Philips IE33	1000 490 - 570	Healthy	10	30±6	3.8±0.4 3.2±0.9		3.4±1.0
Keijzer, 2020 (29)	PLAX A4C	Anteroseptum Inferoseptum	TDI	Zonare Z53	1000	Healthy	10	24-45	3.8(3.4 - 4.0) 5.1(4.5 - 7.2)		
Strachinaru, 2020 (30)	PLAX	Anteroseptum	TDI	Philips IE33	528±22 530±25	Healthy HCM	10 10	37±14 51±11	3.6±0.4 5.3±1.0		
Kvaale, 2020 (17)	Apical	6 walls <sup>b)</sup>	CFWI	GEVU, E9	1000 - 1200	Healthy Myocardial infarction	10 20	34±15 60±6			1.4-2.5 1.8 - 2.5 <sup>b)</sup>
Petrescu, 2020 (15)	PLAX	Anteroseptum	TDI	HD-PULSE	1135±270	Post cardiac transplant	46	54±18			5.0±2.0
Jesus, 2020 (18)	Apical	6 walls, mean	TDI	GEVU, E9 or E95	300 - 465	Healthy Chronic mitral regurg.	40 80	56±11 60±13			1.7(1.5 - 1.8) 2.0(1.5 - 2.2)
Salles, 2021 (7)	Apical	3D, global	CFWI	GEVU, E95	820	Healthy Aortic stenosis	5 10	66±16 64±16			1.6±0.2 2.8±0.8
Espeland (2023), current study	PLAX/A4C	inferoseptum displayed here <sup>d)</sup>	CFWI	GEVU, E95	858±0 858±0 1403 (1213 - 1619)	Healthy Severe aortic stenosis Healthy, HUNT-4	29 13 34	69±10 69±12 64±11	2.6±0.9 4.2±2.1 2.6±1.1		1.3(1.1 - 1.8) 1.4(1.1 - 2.1) 1.3(1.0 - 1.7)

- a) Studies with at least 10 participants, non-abstracts
- b) Significant differences in MWV between healthy and patients in 3 out of 6 tested walls
- c) Values from separate walls can be found in the article

A4C = apical 4 chamber; AK = atrial kick; AVC = aortic valve closure; FPS = frames per second (/s) ; GEVU = GE Vingmed Ultrasound; HCM = hypertrophic cardiomyopathy; MVC = mitral valve closure; PLAX = parasternal long axis